

Quantifying non-stationarity effects on organization of atmospheric turbulent eddy motion by Benford's law



Qinglei Li^{a,b}, Zuntao Fu^{a,*}

^a Laboratory for Climate and Ocean-Atmosphere Studies, Department of Atmospheric and Oceanic Sciences, School of Physics, Peking University, Beijing 100871, China

^b National Meteorological Information Center, China Meteorological Administration, Beijing 100081, China

ARTICLE INFO

Article history:

Received 1 July 2015

Revised 10 September 2015

Accepted 17 September 2015

Available online 25 September 2015

Keywords:

Benford's law

First digit entropy

Multi-scale

Non-stationarity

ABSTRACT

How to quantify the effects of non-stationarity on organization of atmospheric turbulent eddy motions has drawn less attention in recent literatures. Here Benford's law (BL), which states that the first digit (1 through 9) in many datasets follows a monotonically decreasing logarithmic distribution, is used to address this issue for the first time. A quantifier called multi-scale first digit entropy (MFDE) is adopted, which is based on the deviation of BL from the practical first digit distribution of multi-scaled vertical velocity increments, and marked differences are detected in stationary and non-stationary series. The MFDE values of stationary records do not change much with different scales while increase significantly for non-stationary ones as time scales increase. Due to the close relationship between MFDE and the multi-scale Shannon entropy (MSSE), the above results indicate that the non-stationary series are more organized than the stationary ones. Especially, the MFDE can also be used to quantify the different organization degrees of the multi-scaled structures existing in surface vertical velocity records.

© 2015 Elsevier B.V. All rights reserved.

1. Introduction

From a statistical point of view, the time series is considered as stationary when its probabilistic structure is unaffected with a transition in time, and many of the measurements in natural complex geophysical systems are non-stationary when viewed as a whole [1]. The motions in atmospheric boundary layer (ABL) are inherently non-stationary, and records collected in the atmospheric surface layer over land may often be non-stationary. This non-stationarity in ABL is mainly due to wavelike motions, meandering of the wind vector, and numerous unidentified small-scale and meso-scale motions [2,3]. The related concepts of stationarity and the existence and values of integral time scales are central to the ability of analyzing micrometeorological data within the framework of Monin–Obukhov similarity theory and other classical analysis [4]. What is more, the efficiency of the momentum transport systematically increases with increasing non-stationarity [2]. However, issues related to the effects of non-stationarity are not well studied and only recently more attention has been paid [2–10]. Little is known about how to handle or even judge non-stationarity, such that progress cannot be made in determining its consequences, without a better way to characterize it.

The non-stationarity is linked closely to the coexistence of eddies with various scales, especially coherent structures in turbulent flows. In studies of atmospheric turbulence, the coherent structures are described as distinct large-scale fluctuation patterns regularly observed in a given turbulent flows [11]. Turbulent flows in canopies are dominated by such coherent structures of

* Corresponding author. Tel.: +86 10 62767184.
E-mail address: fuzt@pku.edu.cn (Z. Fu).

whole canopy scale [12], which might be responsible for up to 75% of the turbulent fluxes in the atmospheric surface layer [13]. Coherent structures have received close attention from turbulence researchers investigating flow dynamics in the atmospheric boundary layer over the past few decades [11,14–21]. Atmospheric turbulence possesses temporal and spatial scales that range over many orders of magnitude, and the large-scale turbulence (such as coherent structures) is known to have drastic impact on the statistical parameters of the small-scale turbulence [22]. So the degree of organization of complex eddy motions of various scales is really crucial to the non-stationarity of fluid turbulence. Several strategies have been used to quantify the different organization degrees of various-scaled eddy motions [6,10,23]. Wesson et al. [23] used three nonlinear methods including a modified Shannon entropy, wavelet thresholding, and mutual information content to contrast the organization level in the vertical wind velocity time series. They found that motions of various-scaled eddy are more organized within the canopy sub-layer than those in the atmospheric surface layer, and the level of organization increases as the flows in both layers evolve from near-neutral to near-convective conditions. What is more, multi-scale Shannon entropy (MSSE) [6], permutation entropy and statistical complexity [10] have been used to quantify the different organization degrees between stationary and non-stationary vertical wind velocity time series.

However, all above methods are based on the statistics on the probability density distribution of the amplitudes [6,23] or the ordinal patterns [10] in time series, never has the digital information in time series been used to characterize their differences. We should note that digital information is of great importance to characterize specific process. For example, the first digits in many datasets are not uniformly distributed as expected, but heavily right skewed toward the smaller digits. This phenomenon was firstly found by Newcomb in 1881 [24]. Nobody showed interests in this discovery, until Benford [25] investigated some 20 tables of 20,229 numbers and drawn conclusion that the first digit in many data sets follows a monotonically decreasing logarithmic distribution:

$$Q_d = \log_{10}[(d + 1)/d] \quad (1)$$

where $d = 1, 2, \dots, 9$ is the first digit. It was named Benford's law (BL) later by the scientific community. Many scientists in different fields have tried to explain the underlying reason of BL [26–30], but a successful explanation has remained elusive [31,32]. In recent years, most applications of BL are limited to detecting whether particular datasets follow this law [33,34], detecting frauds in election and accounting [35,36], testing physical system transition [37,38]. Only recently, Li and Fu [39] used BL to develop a novel strategy to distinguish stochastic processes and chaotic systems, and found that BL can be applied to detect different dynamics hidden in measurements.

However, all the considered stochastic processes and chaotic systems in the reported work [39] are from idealized models, since the atmospheric turbulent flows are characterized by three-dimensional chaotic motions with different scales and orientations [40], whether this strategy is applicable in boundary layer turbulence? And if so, whether non-stationarity affects the organization degrees of complex eddy motions deserves further research. Herein a new quantifier called MFDE, which based on the deviation of the practical first digit distribution of multi-scale velocity increments from BL, is adopted to handle these problems.

The rest of the paper is organized as follows. In Section 2, a short introduction of the data sets and the analysis methods are given. Detailed results and discussions for stationary and non-stationary vertical wind velocity are shown in Section 2. In Section 4, the conclusions are summarized.

2. Data and methodology

2.1. Data

The vertical velocity records used herein were obtained from a field experiment performed by the State Key Laboratory of Atmospheric Boundary-Layer Physics and Atmospheric Chemistry (LAPC), from 9 to 22 June, 1998. The underlying surface comprises paddy fields and the observation height is 4 m. The instrument used in the experiment is a SAT-211/3k 3-D ultrasonic anemometer, whose sampling frequency is 10 Hz and where each 40,000 sampling points are taken as one record. Typical parts of records can be found in Fig. 1, where stationary and non-stationary records show different features, especially there are dominant larger scale structures in the non-stationary record. More details of the statistical characteristics of the experimental data have been shown elsewhere [5,6,10], and not repeated here for conciseness and clarity. In order to study the non-stationarity effect, some representative series are selected from the datasets after the diagnosis of non-stationarity by means of the space time-index (STI) method [5,6]. The STI is a graphical method and can detect dynamical non-stationarity in a time series. Detailed descriptions of the STI method are presented by Yu et al. [41,42]. A total of 24 vertical velocity time series are selected, and 12 of them are the most non-stationary among the datasets (see NON 1–12 in Table 1), while the other 12 are the most stationary (see STA 1–12 in Table 1). The ensemble-averaged statistical results of 12 samples are shown for each group.

In Table 1, the time when the 24 samples are collected, the mean values of longitudinal wind velocity \bar{u} , the variance of w , σ_w^2 , the mean atmospheric temperature \bar{T} are listed. Typical values of other meteorological variables are calculated and also listed. These variables include the friction velocity,

$$u_* = \left[\overline{u'w'^2} + \overline{v'w'^2} \right]^{1/4}, \quad (2)$$

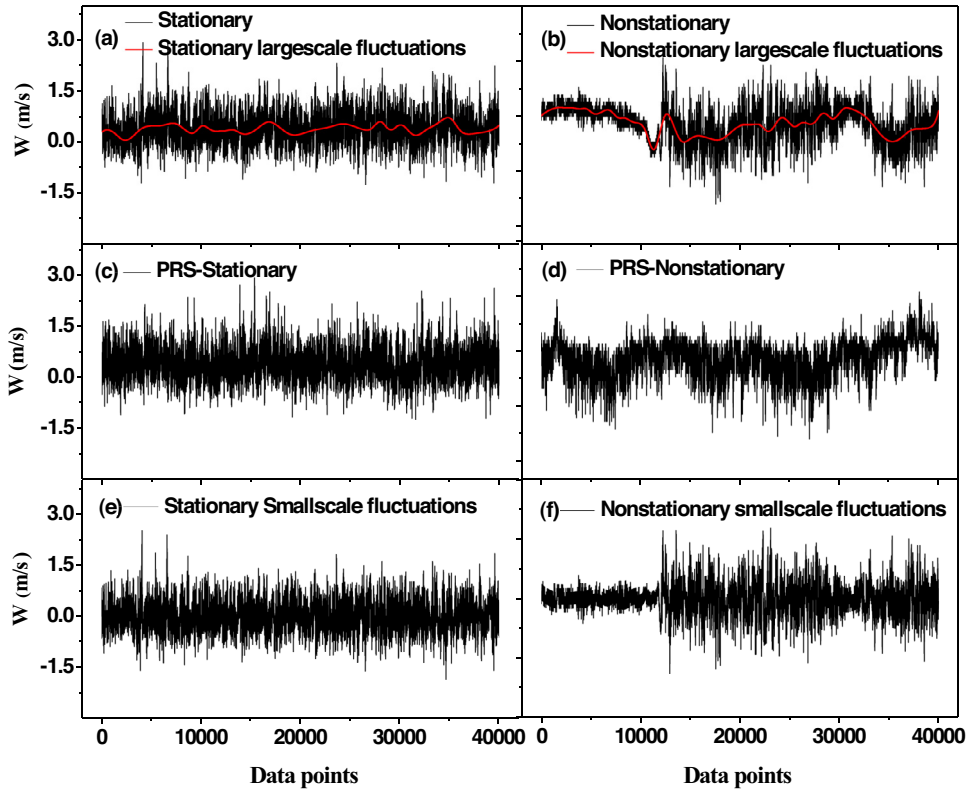


Fig. 1. The normalized segments of (a) stationary vertical velocity time series and its large-scale fluctuations (in red line); (b) non-stationary vertical velocity time series and its large-scale fluctuations (in red line); (c) the stationary series after PRS; (d) the non-stationary series after PRS; (e) the remaining small-scale series from stationary case; and (f) the remaining small-scale series from non-stationary case. (For interpretation of the references to color in this figure legend, the reader is referred to the web version of this article.)

Table 1

The statistical characteristics of the field experiment data for the selected 24 samples: the STA 1–12 represent for the 12 stationary series and the NON 1–12 stand for the 12 non-stationary ones.

Sample	Time	z_m/L	\bar{u} (m/s)	u_* (m/s)	σ_w^2 (m ² /s ²)	H (W/m ²)	\bar{T} (°C)
STA1	06-11,02:00	0.126	2.499	0.180	0.073	-18.029	23.681
STA2	06-11,05:00	0.042	3.088	0.178	0.103	-5.794	23.880
STA3	06-11,06:00	-0.045	3.189	0.222	0.099	12.047	24.231
STA4	06-11,07:00	-0.195	3.775	0.335	0.184	182.840	26.993
STA5	06-11,10:00	-2.073	8.292	0.155	0.185	193.210	29.870
STA6	06-11,13:00	-0.043	6.752	0.228	0.087	12.845	30.853
STA7	06-11,17:00	0.175	2.062	0.131	0.043	-9.845	28.926
STA8	06-11,20:00	-0.215	2.331	0.160	0.068	22.018	26.238
STA9	06-12 11:00	-0.025	-1.520	0.345	0.364	25.302	24.654
STA10	06-12 17:00	0.072	2.135	0.177	0.059	-9.922	24.499
STA11	06-15,03:00	-0.095	2.916	0.214	0.089	23.193	28.630
STA12	06-16,08:00	0.126	2.499	0.180	0.073	-18.029	23.681
NON1	06-09,22:00	1.639	0.740	0.032	0.006	-1.325	24.381
NON2	06-09,23:00	2.501	0.477	0.022	0.002	-0.623	23.832
NON3	06-10,01:00	0.537	-0.043	0.031	0.006	-0.405	23.355
NON4	06-10,04:00	3.437	0.169	0.018	0.002	-0.509	22.683
NON5	06-10,05:00	10.572	0.055	0.015	0.001	-0.823	22.630
NON6	06-10,07:00	-1.888	0.403	0.033	0.005	1.619	23.214
NON7	06-10,22:00	2.942	0.688	0.029	0.003	-1.813	24.866
NON8	06-13,23:00	2.366	-0.328	0.014	0.001	-0.147	22.485
NON9	06-14,02:00	-3.518	0.255	0.005	0.001	0.011	21.776
NON10	06-14,03:00	25.987	-0.075	0.010	0.002	-0.617	21.627
NON11	06-14,04:00	0.444	0.089	0.025	0.002	-0.162	21.151
NON12	06-15,20:00	14.786	-0.046	0.010	0.004	-0.362	30.178

the Obukhov length,

$$L = -\frac{u_*^3 \bar{T}}{\kappa g w' T'}$$
(3)

and the sensible heat flux,

$$H = \rho C_p \overline{w' T'}$$
(4)

where \bar{x} and x' symbolize the time averaging and the deviation from the mean of a measured variable x , u and v are the longitudinal and transversal wind velocities, respectively, T is atmospheric temperature, κ (≈ 0.4) is the von Karman constant, g is the acceleration due to gravity, ρ is the density of air, and C_p is the specific heat capacity of air. Atmospheric stability is denoted by $\xi = z/L$, and usually $-0.02 < \xi < 0.02$ means neutral stratification, $-0.02 \leq \xi$ unstable stratification and $\xi \geq 0.02$ stable stratification. Since the boundary layer turbulence is more fully developed under unstable conditions than stable conditions, most of the 12 stationary series are selected under the unstable stratification, while most of the 12 non-stationary series under stable stratification, as shown in Table 1.

2.2. Methodology

2.2.1. First digit distribution and significance test

For a given time series with data length N , P_d is defined as the observed frequency of digit d . To evaluate the degree of agreement between P_d and Q_d (in Eq. (1)), the Null Hypothesis H_0 is provided as that the observed distribution of the first significant digit in each of the case considered is same as expected on the basis of Benford's law. To test the null hypothesis the Pearson's χ^2 test is carried out as follows:

$$\chi^2(\lambda - 1) = \sum_{d=1}^9 \frac{(NP_d - NQ_d)^2}{NQ_d}$$
(5)

In our case $\lambda = 9$ which means $\lambda - 1 = 8$ degrees of freedom. Under the 95% confidence level, the value of χ^2 is $\chi^2(8) = 15.51$, which is the critical value for acceptance or rejection of H_0 . If the value of the calculated χ^2 is less than the critical value then the null hypothesis is accepted and concludes that the data fits Benford's law [43,44].

2.2.2. MFDE calculation for stationary and non-stationary series

For the chosen stationary and non-stationary vertical velocity time series, the corresponding multi-scale increment series is created as follows:

$$\Delta w = w'(i + n) - w'(i)$$
(6)

where $n = 2^h$ represents multi-scale time lags with $h = 0, 1, 2, \dots, 10$.

According to the definition of Shannon entropy: $S = -P * \log(P)$, MFDE is defined and calculated as follows:

$$MFDE(h) = \frac{\sum_{d=1}^9 P_d^h * \log(P_d^h)}{\sum_{d=1}^9 Q_d * \log(Q_d)}$$
(7)

where Q_d follows Benford's law in Eq. (1) and P_d^h is the actual first digit distribution for the given multi-scale increment series with scale factor h in Eq. (6). According to Eq. (7), the value of MFDE is 1 for Benford's law distributed time series. Higher MFDE values indicate that the first digit distribution in time series tends to be uniform, so the maximum value of MFDE is 1.102 (see Fig. 3) for uniform distributed time series with $P_d^h = 1/9$, $d = 1, 2, 3, \dots, 9$. The minimum value of MFDE is 0 when time series has only one specific digit.

2.2.3. Phase-randomized surrogate (PRS) and empirical mode decomposition (EMD)

In order to confirm the effect of non-stationarity in velocity series on the first digit distribution, the phase-randomized surrogate method (PRS) is performed on the original series [45]. After PRS, both the long-range power-law autocorrelations and the long-range cross-correlation function vanish [46]. PRS involves the following steps: (1) perform Fourier transforms on a velocity fluctuation time series, preserving the amplitudes of the Fourier transform but randomizing the Fourier phases. (2) Perform an inverse Fourier transform to create a surrogate series. This procedure eliminates nonlinear correlations, preserving only the linear features (i.e. two-point correlations) of the original time series [47]. Here PRS is used in both two types of vertical wind velocity series, see Fig. 1c and d.

The empirical mode decomposition (EMD) method is a recent method for analyzing nonlinear and non-stationary processes [48]. The purpose of EMD is used to reduce a complicated data set into a finite and generally small number of intrinsic mode functions (IMFs). It identifies different oscillatory modes in the data based upon their time scales and separates the data into IMFs. Further descriptions of this method are presented in references [49, 50] and are not repeated here. Here EMD is utilized to extract large-scale fluctuations (red line in Fig. 1a and b) in vertical wind velocity series, and to obtain the remaining small-scale fluctuations (Fig. 1e and f). For the non-stationarity series, though the first-order non-stationarity (mean value varies with time) is eliminated after extracting large-scale fluctuations, the second-order non-stationarity (variance changes with time) still exists in the small-scale fluctuations [5], as shown in Fig. 1f.

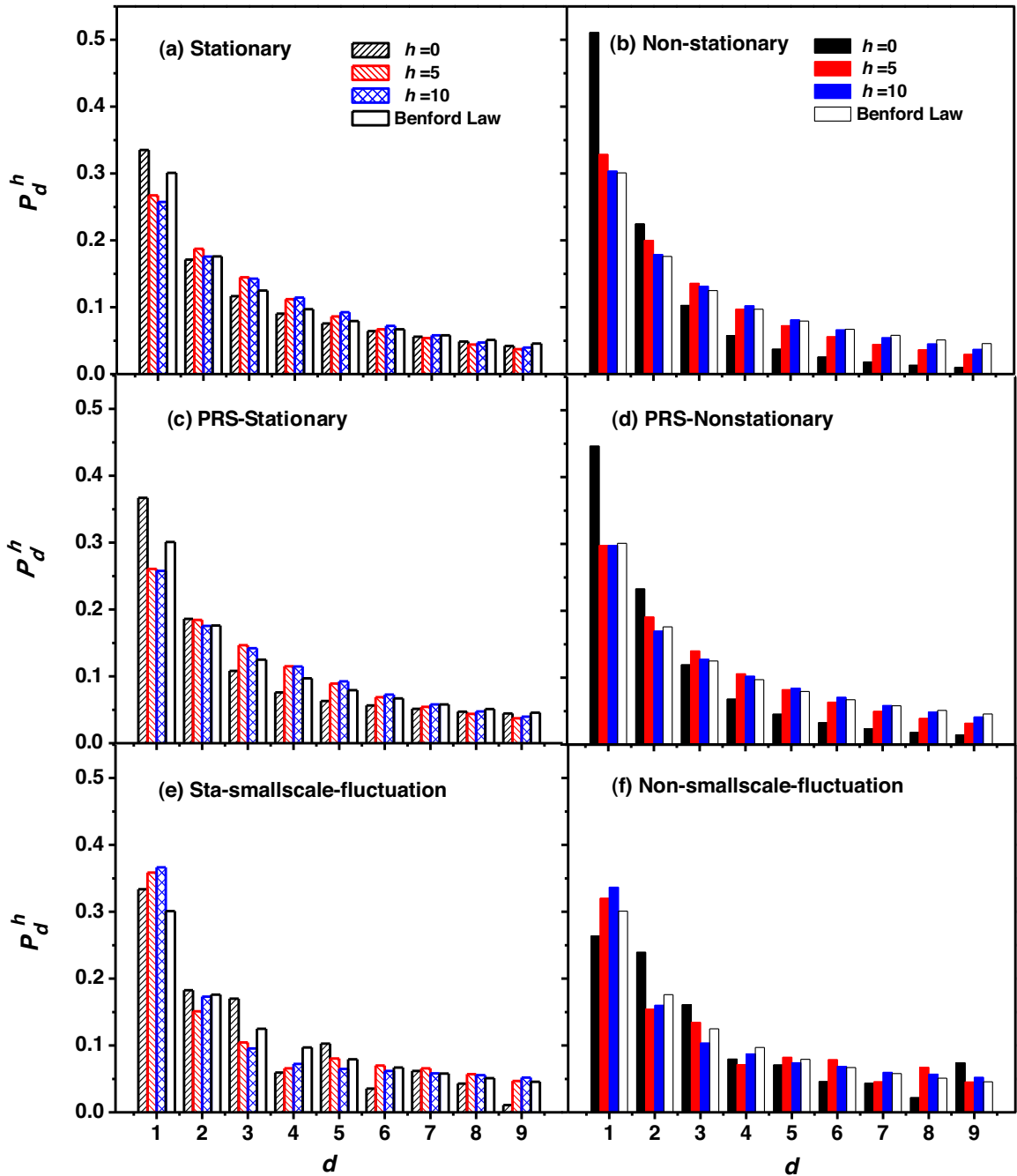


Fig. 2. The first digit distributions of multi-scaled vertical wind velocity increments for: (a) the original stationary time series; (b) the original non-stationary time series; (c) the stationary time series after PRS; (d) the non-stationary time series after PRS; (e) the remaining small-scale series from stationary case; and (f) the remaining small-scale series from non-stationary case.

3. Results and discussions

3.1. First digit distributions of multi-scale increment series

The results of the first digit distribution are shown in Fig. 2. First of all, for the increment series with scale factor $h = 0$, marked differences can be seen between the stationary and non-stationary ones as shown in Fig. 2a and b. The frequency of first digit 1 is about 50% in non-stationary series, far deviating from that of BL distribution ($\chi^2 = 1225 \gg 15.51$), while in stationary series this

frequency is about 33%, and the deviation from BL distribution is smaller ($\chi^2 = 23.2 > 15.51$). Secondly, with the scale factor increases, the frequency of the first digit 1 drops for both two types of time series, but it declines larger for the non-stationary one. Especially, the first digits conform to BL distribution ($\chi^2 = 13.7 < 15.51$) for non-stationary time series with scale factor $h = 10$. It has been demonstrated that the first digit distribution from deterministic chaotic systems deviates from BL with different scales while it does not for the stochastic processes [39]. It is not difficult to understand why the first digit distribution from stationary series changes little with scales, since the atmospheric turbulence is usually fully developed during the day and then some features of the stationary records are more like those from stochastic processes. While some features of the non-stationary series are more like those from the chaotic system, since during the night there are many deterministic components, such as wavelike motions and solitary modes, two-dimensional vortex modes, micro-fronts, intermittent drainage flows, and a host of more complex structures [51].

What is more, since PRS can destroy nonlinear correlations hidden in time series, compared with Fig. 2a and b, Fig. 2c and d show that the PRS procedure affect the results of non-stationary time series more significantly than these of stationary ones. This is consistent with the conclusion that nonlinearity is more notable in non-stationary vertical wind velocity [52]. Lastly, after extracting the large-scale fluctuations through EMD method in both time series, the variations of the first digit distribution with scales become similar for both stationary and non-stationary time series, as shown in Fig. 2e and f. The results indicate that the large-scale modulation is the main factor leading to the different first digit distributions of multi-scaled increments between stationary and non-stationary time series. This is consistent with the results between chaotic systems and stochastic processes in previous work [39].

3.2. MFDE quantifier of non-stationarity effects

To further quantify the differences, the results of MFDE are displayed in Fig. 3. First of all, compared with the non-stationary records, the stationary series has larger MFDE values on the same scale factor; this indicates that the first digit distribution of the velocity increment series is less deviated from BL distribution for stationary time series than for non-stationary ones.

Secondly, with the scale decreasing, the MFDE value increases significantly for non-stationary series while it does not change much for stationary ones. This is because the stationary time series can be regard as stochastic process with less deterministic multi-scale structures, while for non-stationary ones there are more large-scale coherent structures.

Thirdly, the MFDE results for phase-randomized shuffled series are also shown in the Fig. 3. After PRS, the MFDE value for stationary series changes a little, while the MFDE value increases sharply for the non-stationary ones. That is to say, PRS destroy the nonlinear correlations in non-stationary time series [47], but the differences in MFDE between these two types of series still exist. Nonlinear correlation is but not the only factor that affects the first digit distribution of velocity increments over different scales.

Fourthly, after being totally shuffled, MFDE for both types of series reaches the saturation level and does not change with scale varying. The results are consistent with that higher entropy values may be obtained using randomizing techniques to increase the mixing and destroying correlated structures [53].

Lastly, the MFDE for non-stationary small-scale fluctuations is similar with those of the stationary series, indicating that large-scale structure modulation is the main factor leading to the first digit distribution differences, as shown in Fig. 2e and f.

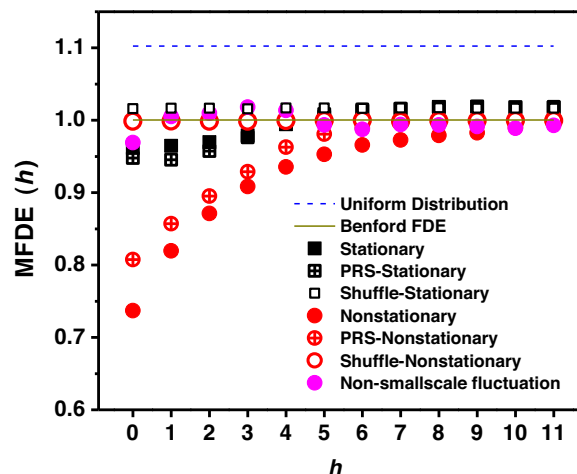


Fig. 3. The results of MFDE for stationary and non-stationary time series, with uniform distribution and Benford's distribution for reference.

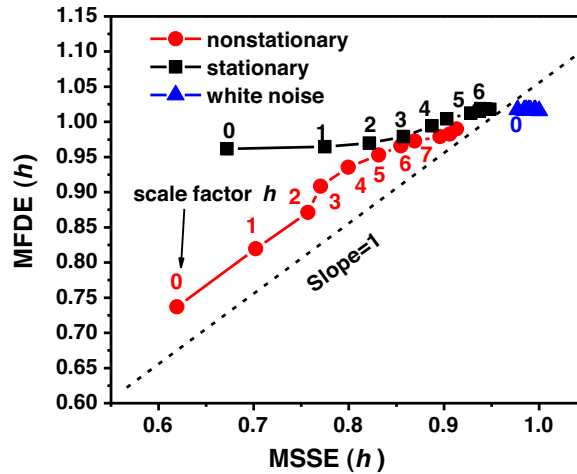


Fig. 4. The relationship between MSSE and MFDE, with the numbers as scale factors.

3.3. Relationship between MFDE and MSSE

In previous research [6], MSSE has been used to quantify different organization degrees between stationary and non-stationary vertical wind velocity records. What is the relationship between MFDE and MSSE? Whether the MFDE can be taken as another indicator to quantify the different organization degrees of the multi-scale structures existing in the stationary and non-stationary surface vertical velocity records? The answers are shown in Fig. 4. Though both MFDE and MSSE increase as the scale factor increases, there are also marked differences between non-stationary and stationary time series: (i) both MFDE and MSSE are larger for the stationary series than the non-stationary at the same scale. (ii) MFDE changes with MSSE nearly linearly (with slope = 1) over whole ranges for non-stationary time series, especially at smaller scales ($h < 3$) and only at larger scales ($h \geq 3$) there is a little deviation from this linear behavior. While for stationary cases, there are predominated different behaviors, the MFDE varies less with MSSE at smaller scales ($h < 3$), and varies linearly with MSSE at larger scales ($h \geq 3$) with a different slope, which is much smaller than 1. (iii) MFDE and MSSE reach their maxima (information saturation) more slowly for non-stationary time series than the stationary counterparts. (iv) MFDE ≈ 1 and MSSE ≈ 1 are obtained for both series after being shuffled, as shown in Fig. 4. In a word, there is a quite good one-to-one correspondence between MFDE and MSSE for both stationary and non-stationary cases, although their features are different. Since multi-scale Shannon entropy has been a useful tool to quantify the organization information of the coherent structures in boundary-layer turbulence dynamics [6], the results indicate how the non-stationarity in the atmospheric turbulent vertical velocity series affects its organization degree can also be quantified by MFDE.

4. Discussion and conclusion

Though a successful explanation has remained elusive for Benford's law [31,32], this work helps to throw a new light on its applications. The different MFDE results for stationary and non-stationary vertical velocity series are consistent with the conclusion that deviations of the first digit distribution from BL vary with different scales in deterministic chaotic systems while not in the stochastic processes [39]. Herein we extend this conclusion from idealized models to practical atmospheric turbulent flows, and exploit that variation of the first digit distribution of velocity increment with scales can be taken to quantify the non-stationarity effects on organization of eddy motions in atmosphere boundary layer.

In atmosphere boundary layer, the stationary and non-stationary series result from different formation mechanisms [5,6,10], and it has been found the non-stationarity often occurs at nocturnal conditions under relatively clear skies [23], because the atmospheric turbulence is usually more fully developed during the day than the night. Turbulence in the very stable regime might be generated primarily by wave-like motions and other small sub-meso motions on time scales of minutes or tens of minutes [40,54] such that equilibrium between the turbulence and deterministic flow is not established [3]. These un-established equilibrium motions cause the interaction between motions of very large scales and small scales [5], and they lead to non-stationarity in the scale regimes analyzed here. Better understanding and quantifying non-stationarity is crucial to explore atmosphere boundary-layer at very stable conditions, especially through time series analysis methods [2,5,6,9,10,52].

It should be mentioned that time series collected in atmosphere boundary-layer can infer plenty of information through different aspects (such as amplitude, phase, the first digit etc.). For example, the amplitude information has been used to quantify different organization degrees by MSSE [6] and the ordinal patterns have used to derive the permutation entropy to quantify the non-stationarity effects [10]. Herein, taking advantage of Benford's law, the first digit in time series can also be applied to quantify non-stationarity effects on organization of atmospheric turbulent eddy motions. From the above analysis, it can be

concluded that quantifiers from the fluctuation amplitude, the ordinal patterns and the first digits will reach similar conclusions in some cases [6,10], but they can also present quantitative and qualitative differences in other cases, such as the relation between MFDE and MSSE for stationary vertical velocity increments over the smaller scales ($h < 3$) in Fig. 4. In order to reach complete understanding of the analyzed process, information from different aspects of the recorded series should be incorporated to derive the full features of the analyzed process.

In summary, the effects of non-stationarity in boundary-layer vertical velocity time series can be reliably quantified by estimating how MFDE changes with the increasing scale factor. It can be concluded that nonlinear correlations and large-scaled structure modulation are main causes of low MFDE values at smaller scales in non-stationary time series. The main advantage of this technique is that it only depends on the first significant digit of an observable. This advantage over the reported non-stationarity analysis [6–10] is very important from the point of view of practical applications, in which accuracy is not very high and uncertainty is unavoidable.

Acknowledgments

The authors acknowledge the supports from the National Natural Science Foundation of China (No. 40975027).

References

- [1] Bendat JS, Piersol AG. Random data: analysis and measurement procedures. New York: John Wiley & Sons; 2000.
- [2] Mahrt L. Boundary-Layer Meteorol 2007;125:245.
- [3] Mahrt L. Boundary-Layer Meteorol 2011;140:343.
- [4] Dias N, Chamecki M, Kan A, Okawa CP. Boundary-Layer Meteorol 2004;110:165.
- [5] Li QL, Fu ZT. Boundary-Layer Meteorol 2013;149:219.
- [6] Fu ZT, Li QL, Yuan NM, Yao ZH. Commun Nonlinear Sci Numer Simul 2014;19:83.
- [7] Beck TW, Housh TJ, Weir JP, Cramer JT, Vardaxis V, Johnson GO, Coburn JW, Malek MH, Mielke M. J Neurosci Methods 2006;156:242.
- [8] Ž Večenaj, De Wekker SFJ. Q J R Meteorol Soc 2015;141:1560. doi:10.1002/qj.2458.
- [9] N. Cullen, K. Steffen, and P. Blanken, Boundary-Layer Meteorol 122, 439 (2007).
- [10] Li QL, Fu ZT. Phys Rev E 2014;89:012905.
- [11] Wilczak J. J Atmos Sci 1984;41:3537.
- [12] Finnigan J. Annu Rev Fluid Mech 2000;32:519.
- [13] Krusche N, De Oliveira A. Boundary-Layer Meteorol 2004;110:191.
- [14] Lemone MA. J Atmos Sci 1976;33:1308.
- [15] Antonia RA, Chambers AJ, Phong-Anant D, Rajagopalan S. Boundary-Layer Meteorol 1979;17:101.
- [16] Thomas C, Foken T. Boundary-Layer Meteorol 2007;123:317.
- [17] Belusic D, Mahrt L. J Geophys Res 2012;117:D09115.
- [18] Shraiman BI, Siggia ED. Nature 2000;405:639.
- [19] Bodenschatz E, Malinowski SP, Shaw RA, Stratmann F. Science 2010;327:970.
- [20] Chian ACL, Miranda RA, Koga D, Bolzan MJA, Ramos FM, Rempel EL. Nonlinear Process Geophys 2008;15:567.
- [21] Campanharo AS, Ramos FM, Macau EE, Rosa RR, Bolzan MJ, Sa LD. Philos Trans A: Math Phys Eng Sci 2008;366:579.
- [22] Muschinski A, Frehlich RG, Balsley BB. J. Fluid Mech 2004;515:319.
- [23] Wesson K, Katul G, Siqueira M. Boundary-layer Meteorol 2003;106:507.
- [24] Newcomb S. Am J Math 1881;4:39.
- [25] Benford F. Proc Am Philos Soc 1938;78:551.
- [26] Goudsmit S, Furry W. Nature 1944;154:800.
- [27] Hill TP. Proc Am Math Soc 1995;123:887.
- [28] Pietronero L, Tosatti E, Tosatti V, Vespignani A. Physica A 2001;293:297.
- [29] Hill TP. Stat Sci 1995;10:354.
- [30] Hill TP. Am Sci 1998;86:358.
- [31] Berger A, Hill TP. Math Intell 2011;33:85.
- [32] Berger A, Hill TP. Probab Surv 2011;8:1.
- [33] Nigrini MJ, Miller SJ. Math Geol 2007;39:469.
- [34] Alves A, Yanasse H, Soma N. Scientometrics 2014;98:173.
- [35] Nigrini MJ, Miller SJ. Audit: J Pract Theory 2009;28:305.
- [36] Mebane WR Jr. Perspect Politics 2004;2:525.
- [37] Sen A, Sen U. Europhys Lett 2011;95:50008.
- [38] Sambridge M, Tkalčić H, Jackson A. Geophys Res Lett 2010;37:L22301.
- [39] Li QL, Fu ZT. PLoS One 2015;10(6):e0129161. doi:10.1371/journal.pone.0129161.
- [40] Ganapathisubramani B, Hutchins N, Hambleton WT, Longmire EK, Marusic I. J Fluid Mech 2005;524:57.
- [41] Yu DJ, Lu WP, Harrison RG. Phys Lett A 1998;250:323.
- [42] Yu DJ, Lu WP, Harrison RG. Chaos 1999;9:865.
- [43] Geyer A, Marti J. Geology 2012;40:327.
- [44] Mir TA. Physica A 2012;391:792.
- [45] Schreiber T, Schmitz A. Phys Rev Lett 1996;77:635.
- [46] Podobnik B, Fu DF, Stanley HE, Ivanov PC. Eur Phys J B 2007;56:47.
- [47] Ashkenazy Y, Ivanov PC, Havlin S, Peng CK, Goldberger AL, Stanley HE. Phys Rev Lett 2001;86(1900).
- [48] Huang NE, Shen Z, Long SR, Wu MC, Shih HH, Zheng Q, Yen NC, Tung CC, Liu HH. Proc R Soc A: Math Phys Eng Sci 1998;454:903.
- [49] Wu Z, Huang NE. Proc R Soc A: Math Phys Eng Sci 2004;460:1597.
- [50] Huang NE, Wu Z. Rev Geophys 2008;46.
- [51] Mahrt L. Annu Rev Fluid Mech 2014;46:23.
- [52] Li QL, Fu ZT, Yuan NM, Xie FH. Physica A 2014;410:9.
- [53] Rosso O, Larrondo H, Martin M, Plastino A, Fuentes M. Phys Rev Lett 2007;99:154102.
- [54] Conangla L, Cuxart J, Soler M. Boundary-Layer Meteorol 2008;128:255.